Annals of the Academy of Romanian Scientists
Online Edition Series on Engineering Sciences
ISSN 2066 – 8570 Volume **7**, Number **1/2015**

3D MODELING OF STRESS FIELDS IN MILLING

Wadii YOUSFI[1], Raynald LAHEURTE[2],
Philippe DARNIS[3], Olivier CAHUC[4], Madalina CALAMAZ[5]

Rezumat. *Având în vedere complexitatea fenomenelor fizice prezente la prelucrarea prin aşchiere, prelucrarea ortogonală a fost configuraţia cea mai exploatată în modelarea analitică a procesului. Această configuraţie nu mai este valabilă dacă avem în vedere orientarea reală în spaţiu a sculei, cum ar fi în cazul procesului de frezare. De-a lungul tăişului parametrii geometrici şi cinematici variază foarte mult şi vectorul viteză a fiecărui punct este foarte sensibil cu poziţia acestuia [1]. Acest studiu include evoluţiile cinematice în spaţiul de lucru, cu pante semnificative privind viteza de lucru, în configuraţia de prelucrare 3D şi pentru fiecare din zonele de forfecare. Gradientul de viteză generează deplasări suplimentare ale aşchiei, în trei dimensiuni, prin urmare, există o nouă componentă a forţei şi se remarcă apariţia momentelor de aşchiere. Acest studiu prezintă o scurtă descriere a modelului de aşchiere ortogonală urmată de determinarea câmpului de viteze în fiecare zonă de forfecare. Din expresia generală a vectorului de viteză, sunt determinate contribuţiile variaţiilor cinematice asupra stării de tensiune şi a evoluţiei acesteia între cele două puncte extreme ale muchiei aşchietoare.*

Abstract. *Given the complexity of the physical phenomena present in machining, orthogonal cutting was the most exploited configuration in the analytical modelling of cutting. This configuration is no longer valid if we consider the orientations of the tool in space such as the milling process. A along the cutting edge the geometric and kinematic parameters vary greatly and the speed vector of each point is very sensitive to the position [1]. This study incorporates the kinematic evolutions in the volume, with significant gradients of speeds, in 3D machining configuration and this in each shear zone. These gradients velocity generate additional displacements of the chip, in three dimensions, therefore a new force component with the appearance of cutting moments. This study presents a brief description of orthogonal cutting model developed followed by the determination of the velocity field in each shear zone. From the overall expression of the velocity vector, the contributions of the kinematic variations to the strain and the strain rate between the two extreme points of the edge are determined.*

Keywords: Orthogonal cutting, milling, velocity gradients, strain gradients

1. Introduction

This study consists to determine the velocity of each point in each shear zone considering the boundary conditions at the tool-material interface. The strain is

[1]PhD Student, MPI-I2M, Universty of Bordeaux, Bordeaux, France (wadii.yousfi@u-bordeaux.fr).
[2]PhD, MPI, I2M, Universty of Bordeaux, Bordeaux, France (raynald.laheurte@u-bordeaux.fr).
[3]Prof, MPI, I2M, Universty of Bordeaux, Bordeaux, France (philippe.darnis@u-bordeaux.fr).
[4]Prof, MPI, I2M, Universty of Bordeaux, Bordeaux, France (olivier.cahuc@u-bordeaux.fr).
[5]PhD, MPI, I2M, ENSAM, Bordeaux, France (madalina.calamaz@ensam.eu).

calculated by a spatial derivation of displacements generated. The strain rate is calculated by a spatial derivation of the velocity fields. The difference in velocity along the cutting edge generates strain gradients and strain rates gradients. This study deals with the determination of the strain gradients and strain rate gradients generated by the difference of velocities along the cutting edge.

2. Basic cutting model

In orthogonal cutting configuration and in the three cutting areas [2], [3] (primary, secondary and tertiary shear zones) the displacements, the strains and the strain rates are determined from the trajectory of each particle in the material. An element through the primary shear zone is assumed to follow an hyperbolic trajectory [4]. The component of the velocity parallel to the shear plane is assumed to be constant. A new velocity component perpendicular to the cutting surface is considered in the secondary shear zone (Fig. 8). Its value varies linearly until it vanishes along the tool-chip contact length. A linear variation of the chip velocity at the interface is considered. The acuity of the tool generates a displacement of the part of material along the rake face by plastically deforming. An elastic spring back occurs at the free surface of the machined material. The section of the tool in the calculation map is represented by a circular arc whose two asymptotes are the flank face and the rake face. A balance power between the area above and below the stagnation point is used to determine the exact position of this point.

3. Study of the primary shear zone

3.1. Displacement and velocity field carried by x_φ

The orientation in space of the cutting edge generates a significant speed gradient dV_N of the velocity V_N (Fig. 1) [1]. Along the cutting edge two extreme points $P_{2,\inf}$ and $P_{2,\sup}$ are defined, (Fig. 2).

The velocity field expression carried by x_φ and normal to the shear zone is of the form:

$$V_N\left(y_\phi, z_\phi\right) = \frac{dV_N}{a_p'.l}.y_\phi.z_\phi + \frac{V_{N,P_{2,\inf}}}{l}.y_\phi \ . \tag{1}$$

The time considered for the calculation of the displacement and strain is equal to the time for an element to cross the entire primary shear zone. This time is calculated with the smallest normal speed (the greatest time) and is defined by:

$$t = \frac{h_{moy}}{V_{N,P_{2,\inf}}} \ . \tag{2}$$

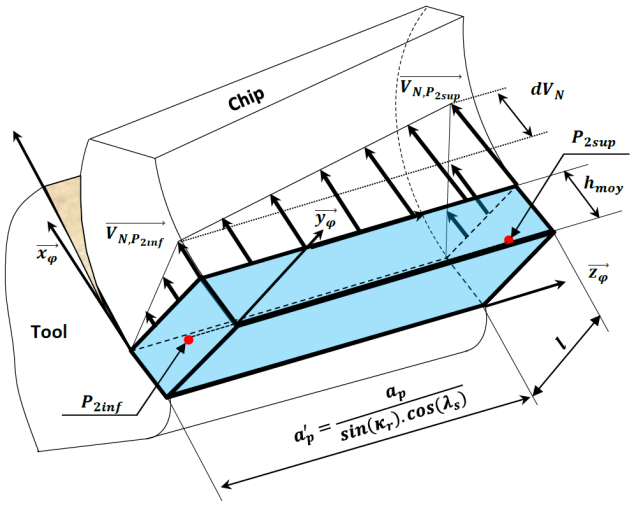

Fig. 1. The velocity distribution carried by x_φ .

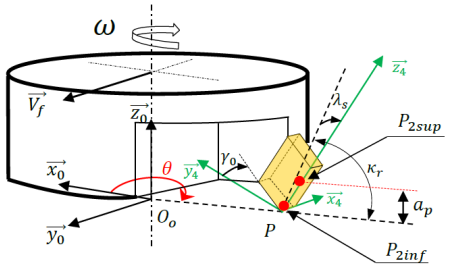

Fig. 2. Orientation of insert in the Milling.

The total displacement along x_φ is determined by:

$$U_{x_\phi}\left(y_\phi, z_\phi, t\right) = \frac{dV_N}{a_p'.l}.y_\phi.z_\phi.t + \frac{V_{N,P_{2,\inf}}}{l}.y_\phi.t \quad . \tag{3}$$

3.2. Displacement and velocity field carried by y_φ

At the end of the primary shear zone $(x_\varphi = h_{moy})$, the sliding velocity varies linearly from point $P_{2,\inf}$ to point $P_{2,\sup}$. This velocity is considered void on the side of the work piece $(x_\varphi = 0)$.

The velocity field carried by y_ϕ is expressed by:

$$V_S\left(x_\phi, z_\phi\right) = \frac{dV_S}{a_p'.h_{moy}}.x_\phi.z_\phi + \frac{V_{S,P_{2,\inf}}}{h_{moy}}.x_\phi \quad . \tag{4}$$

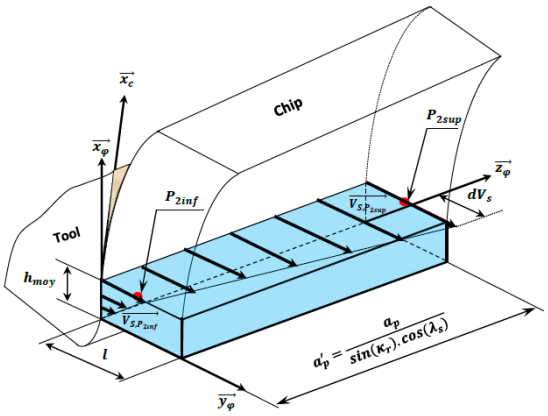

Fig. 3. The velocity distribution carried by y_ϕ.

The displacement expression carried by y_ϕ is defined by:

$$U_{y_\phi}\left(x_\phi, z_\phi, t\right) = \frac{dV_S}{a'_p.h_{moy}}.x_\phi.z_\phi.t + \frac{V_{S,P_{2,\inf}}}{h_{moy}}.x_\phi.t \quad . \tag{5}$$

3.3. Displacement and velocity field carried by z_φ

Cutting edge inclination angle generates the appearance of a velocity component carried by the cutting edge (Fig. 4) along the axis z_ϕ. This velocity is equal to zero at the interface of primary shear zone – workpiece $(x_\phi = 0)$ and its value is maximum at the end of this zone.

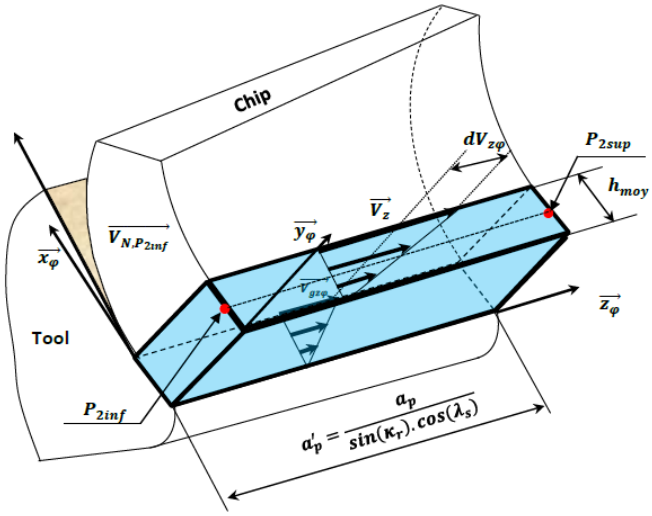

Fig. 4. The velocity distribution carried by z_ϕ.

Starting from the surface contact between the material and the tool $(y_\varphi = 0)$ toward the free surface of the primary shear zone, the new velocity component varies linearly.

The minimum value at the interface depends on the sliding velocity and therefore the friction coefficient. The velocity field expression carried by z_ϕ is determined by:

$$V_{z_\phi}\left(x_\phi, y_\phi\right) = \frac{(V_Z - V_{gZ})}{l.h_{moy}}.x_\phi.y_\phi + \frac{V_{gZ}}{h_{moy}}.x_\phi \ . \tag{6}$$

The total displacement in the primary shear zone is expressed by:

$$U_{z\phi}\left(x_\phi, y_\phi, t\right) = \frac{(V_Z - V_{gZ})}{l.h_{moy}}.x_\phi.y_\phi.t + \frac{V_{gZ}}{h_{moy}}.x_\phi.t \ . \tag{7}$$

3.4. Calculation of the strain and the strain rate in the primary shear zone

The spatial derivation of the displacement field in the primary shear zone gives the strain tensor, and the generalized value of strain is determined by:

$$\varepsilon_{éq,zp} = \sqrt{\varepsilon_{1éq,zp} + \varepsilon_{2éq,zp} + \varepsilon_{3éq,zp}} \ , \tag{8}$$

with:
$$\varepsilon_{1éq,zp} = \frac{1}{3}.\left(\frac{dV_N}{a_p^{'}.l}.z_\phi.t + \frac{V_{N,P_{2,\inf}}}{l}.t + \frac{dV_S}{a_p^{'}.h_{moy}}.z_\phi.t + \frac{V_{S,P_{2,\inf}}}{h_{moy}}.t\right)^2 \ , \tag{9}$$

$$\varepsilon_{2éq,zp} = \frac{1}{3}.\left(\frac{dV_N}{a_p^{'}.l}.y_\phi.t + \frac{dV_Z}{l.h_{moy}}.y_\phi.t + \frac{V_{gZ}}{h_{moy}}.t\right)^2 , \tag{10}$$

$$\varepsilon_{3éq,zp} = \frac{1}{3}.\left(\frac{dV_Z}{h_{moy}.l}.x_\phi.t + \frac{dV_S}{a_p^{'}.h_{moy}}.x_\phi.t\right)^2 \ . \tag{11}$$

The kinematic and geometric parameters are given in Table 1, and the variation of the equivalent strain along the cutting edge for different cutting angles is shown in Fig. 5.

This variation shows a large strain gradient along the cutting edge, its value is greater of 10% at the point $P_{2,\sup}(z_\varphi = a_p^{'})$ compared to the value at the point $P_{2,\inf}(z_\varphi = 0)$. This difference corresponds to the "additional strain" generated by the orientation of the insert in space.

Table 1 Geometric and kinematic parameters of the study

$\omega(rad.s^{-1})$	a_p	R_0	κ_r	γ_0	λ_s
200	2 mm	25 mm	45°	6°	6°

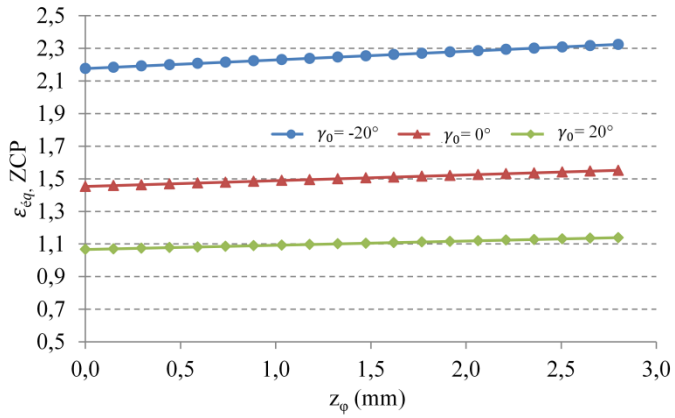

Fig. 5. Variation of the equivalent strain in the primary shear zone along the cutting edge.

The strain rate tensor is obtained by the derivation of the velocity field and the generalized strain rate is defined by:

$$\dot{\varepsilon}_{éq,zp} = \sqrt{\dot{\varepsilon}_{1éq,zp} + \dot{\varepsilon}_{2éq,zp} + \dot{\varepsilon}_{3éq,zp}} \quad , \tag{12}$$

with,

$$\dot{\varepsilon}_{1éq,zp} = \frac{1}{3}.\left(\frac{dV_N}{a_p'.l}.z_\phi + \frac{V_{N,P_{2,\inf}}}{l} + \frac{dV_S}{a_p'.h_{moy}}.z_\phi + \frac{V_{S,P_{2,\inf}}}{h_{moy}} \right)^2 \quad , \tag{13}$$

$$\dot{\varepsilon}_{2éq,zp} = \frac{1}{3}.\left(\frac{dV_N}{a_p'.l}.y_\phi + \frac{dV_Z}{l.h_{moy}}.y_\phi + \frac{V_{gZ}}{h_{moy}} \right)^2 \quad , \tag{14}$$

$$\dot{\varepsilon}_{3éq,zp} = \frac{1}{3}.\left(\frac{dV_{Z4}}{h_{moy}.l}.x_\phi + \frac{dV_S}{a_p'.h_{moy}}.x_\phi \right)^2 \quad . \tag{15}$$

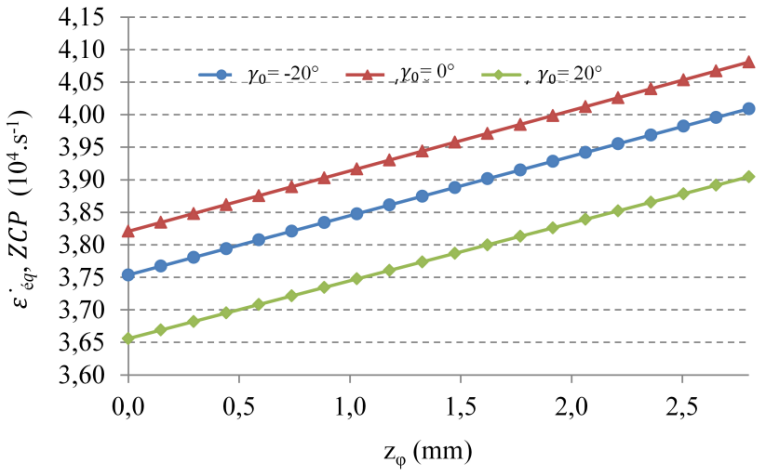

Fig. 6. Variation of the equivalent strain rate in the primary shear zone along the cutting edge.

For the same geometrical parameters given in Table 1, the variation of the equivalent strain rate along the cutting edge for different cutting angles is shown in Fig. 6. The strain rate gradient calculated along the cutting edge is significant and the evolution is comparable to the strain behaviour. The strain rate at the point $P_{2,\sup}(z_\varphi = a_p^{'})$ is greater of 7% from the value at the point $P_{2,\inf}(z_\varphi = 0)$.

4. Study of the secondary shear zone

4.1. Displacement and velocity field carried by x_c

The secondary shear zone is assumed as a triangular volume (Fig. 7). The velocity carried by x_c varies linearly along the axis normal to the cutting face. Its value varies from the sliding velocity at the interface to a value equal to the speed chips at the surface between the shearing zone and the rest of the chip (plan $z_c x_c^{'}$). Along the axis x_c (contact of the chip with cutting face) the velocity varies from zero for $x_c = 0$ to a value equal to the chip velocity at the output of the contact area. Starting from the point $P_{2,\inf}$ to $P_{2,\sup}$ this velocity component increases linearly.

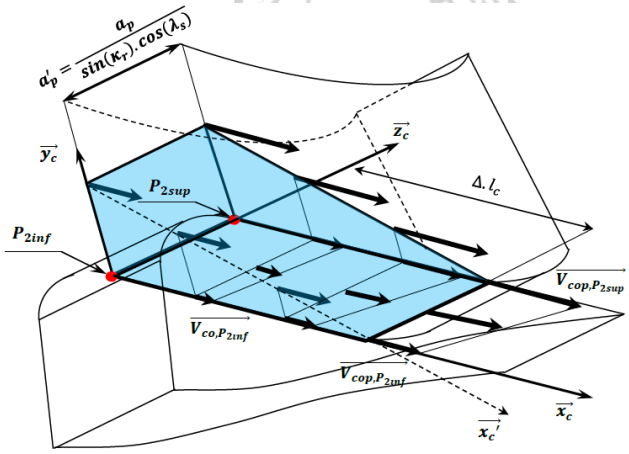

Fig. 7. The velocity distribution carried by x_c.

The velocity field expression carried by x_c is expressed by:

$$V_{x_c}(x_c, y_c, z_c) = \frac{dV_{cop}}{a_p^{'}.\delta.t_2}.y_c.z_c + \frac{dV_{cop}}{a_p^{'}.\Delta.l_c}.x_c.z_c + \frac{V_{cop,P_{2\inf}}}{\Delta.l_c}.x_c + \frac{V_{cop,P_{2\inf}}}{\delta.t_2}.y_c . \quad (16)$$

The total displacement carried by x_c in the secondary shear zone is determined by:

$$U_{x_c}(x_c, z_c, t) = \left(\frac{dV_{cop}}{a_p^{'}}.z_c - \frac{dV_{cop}}{a_p^{'}.\Delta.l_c}.x_c.z_c - \frac{V_{cop,P_{2\inf}}}{\Delta.l_c}.x_c + V_{cop,P_{2\inf}} \right).t \ . \quad (17)$$

4.2. Displacement and velocity field carried by y_c

The trajectory of an element incoming in the secondary shear zone is considered curvilinear. A new component of velocity V_y normal to the cutting face varies from a maximum value at the beginning of this zone to zero at the end. The Fig. 8 shows the variation of this velocity between the two extreme points along the edge. The expression of the velocity field carried by y_c is defined by:

$$V_{y_c}(x_c, z_c) = \frac{dV_y}{a_p'}.z_c - \frac{dV_y}{a_p'.\Delta.l_c}.x_c.z_c - \frac{V_{y,P_{2\inf}}}{\Delta.l_c}.x_c + V_{y,P_{2\inf}} \tag{18}$$

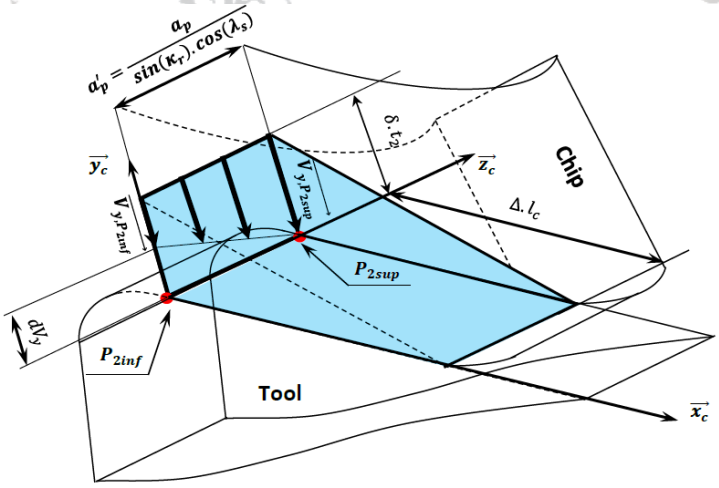

Fig. 8. The velocity distribution carried by y_c.

The displacement field expression carried by y_c is expressed by:

$$U_{y_c}(x_c, z_c, t) = \frac{dV_y}{a_p'}.\left(1 - \frac{x_c}{\Delta l_c}\right).z_c.t\,. \tag{19}$$

4.3. Displacement and velocity field carried by y_c

The velocity component carried by the cutting edge varies linearly along the thickness of the secondary shear zone. It varies from a value equal to the slip velocity across the cutting face to a maximum value at the inlet of the secondary shear zone (Fig. 9).

The velocity field expression carried by z_c is determined by:

$$V_{Z_c}(x_c, y_c) = -\frac{dV_Z}{\Delta.l_c.\delta.t_2}.x_c.y_c + \frac{dV_Z}{\delta.t_2}.y_c + V_g\,. \tag{20}$$

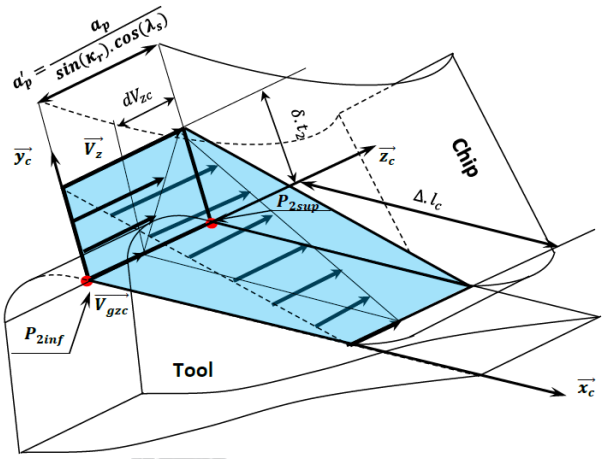

Fig. 9. The velocity distribution carried by z_c

The displacement field expression carried by z_c is defined by:

$$U_{z_c}(x_c, y_c, t) = \frac{dV_Z . y_c}{\delta.t_2} . \left(1 - \frac{x_c}{\Delta l_c}\right).t \,. \tag{21}$$

4.4. Calculation of the strain and the strain rate in the secondary shear zone

The equivalent strain is determined by:

$$\varepsilon_{éq,zs} = \sqrt{\varepsilon_{1éq,zs} + \varepsilon_{2éq,zs} + \varepsilon_{3éq,zs} + \varepsilon_{4éq,zs} + \varepsilon_{5éq,zs}} \,, \tag{22}$$

with,

$$\varepsilon_{1éq,zs} = \frac{8}{27} . \left(- \frac{dV_{cop}}{a'_p . \Delta . l_c} . z_c . t - \frac{V_{cop,P_{2,\inf}}}{\Delta . l_c} . t \right)^2 , \tag{23}$$

$$\varepsilon_{2éq,zs} = \frac{1}{3} . \left(\frac{dV_y}{a'_p . \Delta . l_c} . z_c . t \right)^2 , \tag{24}$$

$$\varepsilon_{3éq,zs} = \frac{1}{3} . \left(- \frac{dV_{cop}}{a'_p . \Delta . l_c} . x_c . t + \frac{dV_{cop}}{a'_p} . t - \frac{dV_Z}{\delta . t_2 . \Delta . l_c} . y_c . t \right)^2 , \tag{25}$$

$$\varepsilon_{4éq,zs} = \frac{4}{27} . \left(- \frac{dV_{cop}}{a'_p . \Delta . l_c} . z_c . t - \frac{V_{cop,P_{2,\inf}}}{\Delta . l_c} . t \right)^2 , \tag{26}$$

$$\varepsilon_{5éq,zs} = \frac{1}{3} . \left(\frac{dV_y}{a'_p} . \left(1 - \frac{x_c}{\Delta . l_c}\right) . t + \frac{dV_Z}{\delta . t_2} . t - \frac{dV_Z}{\delta . t_2 . \Delta . l_c} . x_c . t \right)^2 . \tag{27}$$

For the kinematic and geometric parameters given in Table 1, the variation of the equivalent strain for different cutting angles is shown in Fig. 10.

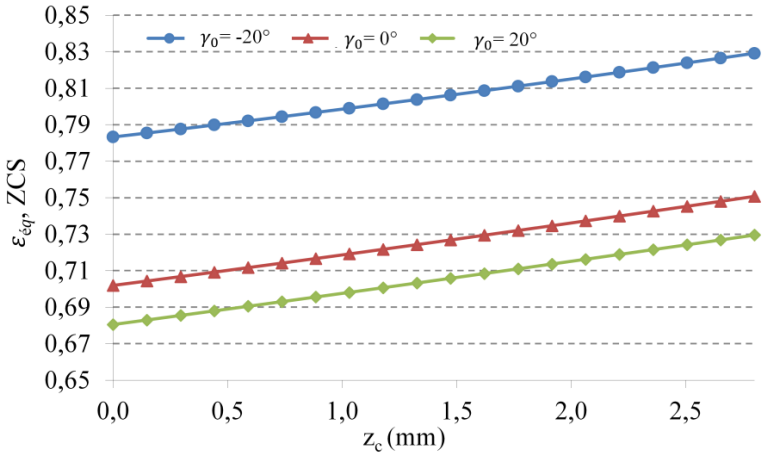

Fig. 10. Variation of the equivalent strain in the secondary shear zone along the cutting edge.

The equivalent strain decreases from negative cutting angles to positive angles. As the primary shear zone, this variation shows a large strain gradient along the cutting edge. Its value is greater on average 7% at point $P_{2,\sup}(z_c = a_p')$ compared to the value at the point $P_{2,\inf}(z_\varphi = 0)$ and this difference corresponds to the "additional strain ". The generalized strain rate is defined by:

$$\dot{\varepsilon}_{éq,zs} = \sqrt{\dot{\varepsilon}_{1éq,zs} + \dot{\varepsilon}_{2éq,zs} + \dot{\varepsilon}_{3éq,zs} + \dot{\varepsilon}_{4éq,zs} + \dot{\varepsilon}_{5éq,zs}}\,, \tag{28}$$

with,

$$\dot{\varepsilon}_{1éq,zs} = \frac{8}{27}.\left(\frac{dV_{cop}}{a_p'.\Delta.l_c}.z_c + \frac{V_{cop,P_{2,\inf}}}{\Delta.l_c}\right)^2, \tag{29}$$

$$\dot{\varepsilon}_{2éq,zs} = \frac{1}{3}.\left(\frac{dV_{cop}}{a_p'.\delta.t_2}.z_c + \frac{V_{cop,P_{2\inf}}}{\delta.t_2} - \frac{dV_y}{a_p'.\Delta.l_c}.z_c - \frac{V_{y,P_{2\inf}}}{\Delta.l_c}\right)^2, \tag{30}$$

$$\dot{\varepsilon}_{3éq,zs} = \frac{1}{3}.\left(\frac{dV_{cop}}{a_p'.\delta.t_2}.y_c + \frac{dV_{cop}}{a_p'.\Delta.l_c}.x_c - \frac{dV_Z}{\delta.t_2.\Delta.l_c}.y_c\right)^2, \tag{31}$$

$$\dot{\varepsilon}_{4éq,zs} = \frac{4}{27}.\left(\frac{dV_{cop}}{a_p'.\Delta.l_c}.z_c + \frac{V_{cop,P_{2,\inf}}}{\Delta.l_c}\right)^2, \tag{32}$$

$$\dot{\varepsilon}_{5éq,zs} = \frac{1}{3}.\left(-\frac{dV_y}{a_p'.\Delta.l_c}.x_c + \frac{dV_y}{a_p'} - \frac{dV_Z}{\delta.t_2.\Delta.l_c}.x_c + \frac{dV_Z}{\delta.t_2}\right)^2. \tag{33}$$

The variation of the equivalent strain rate in the secondary shear zone and along the cutting edge z_c for different cutting angles γ_0 is shown in Fig. 11:

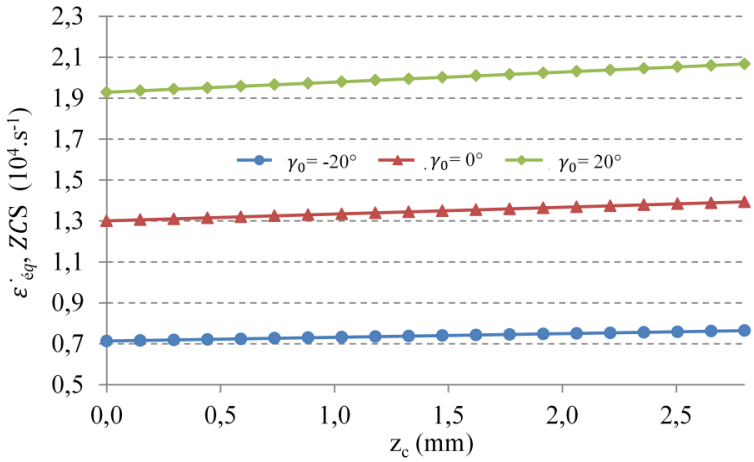

Fig. 11. Variation of the equivalent strain rate in the secondary shear zone along the cutting edge.

The strain rate is lower than in the primary shear zone and its variation, from the point $P_{2,\text{inf}}$ to $P_{2,\text{sup}}$ is similar to the primary shear zone. This difference of the strain rate along the edge is equal to 7%.

Conclusions

This paper presents a new detailed approach to calculate strain and strain rates in both shear zones during the cutting process and for a milling configuration. The orientation of the insert in the space creates strong velocity gradients along the cutting edge. These gradients directly influence the strain and strain rate fields. 7% of variation are calculated between the two extreme points of the cutting edge and thus a significant difference in the stress fields and cutting mechanical actions.

Acknowledgment

This work was conducted as part of the working group "Manufacturing'21" which includes 18 French research laboratories. The studied areas are: modelling tool / material interactions, the mechanical behaviour of articulated structures, the digital factory, innovative and sustainable processes.

Notations

$\left(\vec{x}_\phi, \vec{y}_\phi, \vec{z}_\phi\right), \left(\vec{x}_c, \vec{y}_c, \vec{z}_c\right)$: Coordinate systems respectively associated with the primary and secondary shear zone.

$V_N, V_{N,P_{2,\inf}}, V_{N,P_{2,\inf}}, V_S, V_{S,P_{2,\inf}}, V_{S,P_{2,\inf}}$ **:** Normal and sliding velocities in the primary shear zone at point $P_{2,\inf}$ and $P_{2,\sup}$**.**

$V_{Z_\varphi}(V_{Z_c}), V_Z, V_{gZ}(V_g)$ **:** Velocity components carried by the cutting edge, maximum velocity, interfacial tool-chip velocity.

$V_{x_c}, V_{cop,P_{2,\inf}}, V_{cop,P_{2,\sup}}, V_{y_c}, V_{y,P_{2,\inf}}, V_{y,P_{2,\sup}}$ **:** Velocity component carried by x_c and y_c to the point $P_{2,\inf}$ and $P_{2,\sup}$**.**

$dV_N, dV_S, dV_Z, dV_{cop}, dV_y$ **:** Maximum velocity differences for the velocity fields $V_N, V_S, V_Z, V_{cop}, V_y$**.**

$U_{x_\varphi}, U_{y_\varphi}, U_{z_\varphi}, U_{x_c}, U_{y_c}, U_{z_c}$ **:** Displacement fields respectively in R_φ et R_c.

$\varepsilon_{éq,Zp}, \varepsilon_{éq,Zs}, \dot{\varepsilon}_{éq,Zp}, \dot{\varepsilon}_{éq,Zs}$ **:** Strain and generalized strain rate in primary and secondary shear zone.

$l, h_{moy}, a_p, a_p^{'}, R_0, t$ **:** Length of the ZCP , thickness of the ZCS, depth of cut, real depth of cut on the edge, the tool radius, calculation time.

$\kappa_r, \gamma_0, \lambda_s, \Delta.l_c, \delta.t_2$ **:** Orientation angles of the insert, length of the contact tool/material.

REFERENCES

[1] W. Yousfi, "*3D Kinematic fields studies in milling*", International Conference on Manufacturing System, pp 163-198. Bucarest, 2014.

[2] M.E. Merchant, "*Mechanics of the metal cutting process, I: orthogonal cutting*", Journal of Applied Physics, Vol. N°16, 1945, pp. 267-275.

[3] P.L.B. Oxley, "*Mechanics of the metal cutting*", International Journal of Machine Tool Design and Research, Vol. N°1, 1961, pp. 89-94.

[4] F. Dargnat, Ph. Darnis, O. Cahuc, "*Analytical modelling of cutting phenomena improvements with a view to drilling modelling*", International Journal of Machining and Machinability of Materials, Vol. N°5, 2009, pp. 176-206.

[5] A. Molinari, D. Dudzinski, "*Stationary shear band in high-speed machining*", C.R. Acad. Science Paris, Vol. 3l5 (II), 1992, p.399-405.

[6] G. Albert, R. Laheurte, J-Y K'nevez, Ph. Darnis, O. Cahuc.,"*Experimental milling moment in orthogonal cutting condition: to an accurate energy balance*", Journal of Advanced Manufacturing Technology, Vol. N°55, 2011, pp. 843-854.

[7] S. Engin, Y. Altintas. "*Mechanics and dynamics of general milling cutters. Part II: inserted cutters*", International Journal of Machine Tools & Manufacture, Vol. N°41, 2001, pp. 2213-2231.

[8] Sandvik-Coromant, "*Fraisage principes*", Techniques de l'ingénieur, BM7082, 2001, pp. 1-21.